Review Article
Altered sympathetic nervous system signaling in the diabetic heart: emerging targets for molecular imaging

James T Thackeray[1,2], Rob S Beanlands[1,2], Jean N DaSilva[1,2]

[1]Molecular Function & Imaging Program, National Cardiac PET Centre, University of Ottawa Heart Institute; [2]Department of Cellular & Molecular Medicine, Faculty of Graduate and Postdoctoral Studies, University of Ottawa, Canada

Abstract: Diabetes is commonly associated with increased risk of cardiovascular morbidity and mortality. Perturbations in sympathetic nervous system (SNS) signaling have been linked to the progression of diabetic heart disease. Glucose, insulin, and free fatty acids contribute to elevated sympathetic nervous activity and norepinephrine release. Reduced left ventricular compliance and impaired cardiac function lead to further SNS activation. Chronic elevation of cardiac norepinephrine culminates in altered expression of pre- and post-synaptic sympathetic signaling elements, changes in calcium regulatory proteins, and abnormal contraction-excitation coupling. Clinically, these factors manifest as altered resting heart rate, depressed heart rate variability, and impaired cardiac autonomic reflex, which may contribute to elevated cardiovascular risk. Development of molecular imaging probes enable a comprehensive evaluation of cardiac SNS signaling at the neuron, postsynaptic receptor, and intracellular second messenger sites of signal transduction, providing mechanistic insights into cardiac pathology. This review will examine the evidence for abnormal SNS signaling in the diabetic heart and establish the physiological consequences of these changes, drawing from basic biological research in isolated heart and rodent models of diabetes, as well as from clinical reports. Particular attention will be paid to the use of molecular imaging approaches to non-invasively characterize and evaluate sympathetic signal transduction in diabetes, including pre-synaptic norepinephrine reuptake assessment using [11]C-*meta*-hydroxyephedrine (^{11}C-HED) with PET or ^{123}I-metaiodobenzylguanidine (^{123}I-MIBG) with SPECT, and post-synaptic β-adrenoceptor density measurements using CGP12177 derivatives. Finally, the review will attempt to define the future role of these non-invasive nuclear imaging techniques in diabetes research and clinical care.

Keywords: Sympathetic neuronal imaging, SNS signaling, norepinephrine, β-adrenoceptor, norepinephrine reuptake transporter

Introduction

Diabetes is a prominent risk factor for the development of cardiovascular disease. Patients with diabetes carry 4 times greater risk of cardiovascular mortality, and constitute a disproportionate cohort of large scale heart failure studies. The interaction between diabetes and heart failure is diverse, with many pathways having been implicated. One factor in common between the conditions is impairment of the cardiac sympathetic nervous system (SNS), characterized initially by hyperactivity and elevated norepinephrine spillover, eventually culminating in sympathetic denervation and reduced capacity for norepinephrine release. Acute sympathetic activation evokes increased heart rate and contractility, whereas chronic activation can depress SNS sensitivity.

Continued advances in molecular imaging have led to the characterization of multiple radiotracers for the interrogation of the cardiac SNS. In a preclinical setting, longitudinal non-invasive imaging studies of sympathetic regulation during the development of diabetes and subsequent left ventricular dysfunction can provide important mechanistic insights into cardiac pathology. Long-term clinical application of imaging techniques could be used to stratify cardiovascular risk among diabetic patients.

Sympathetic nervous system signal transduction

The autonomic nervous system is the primary
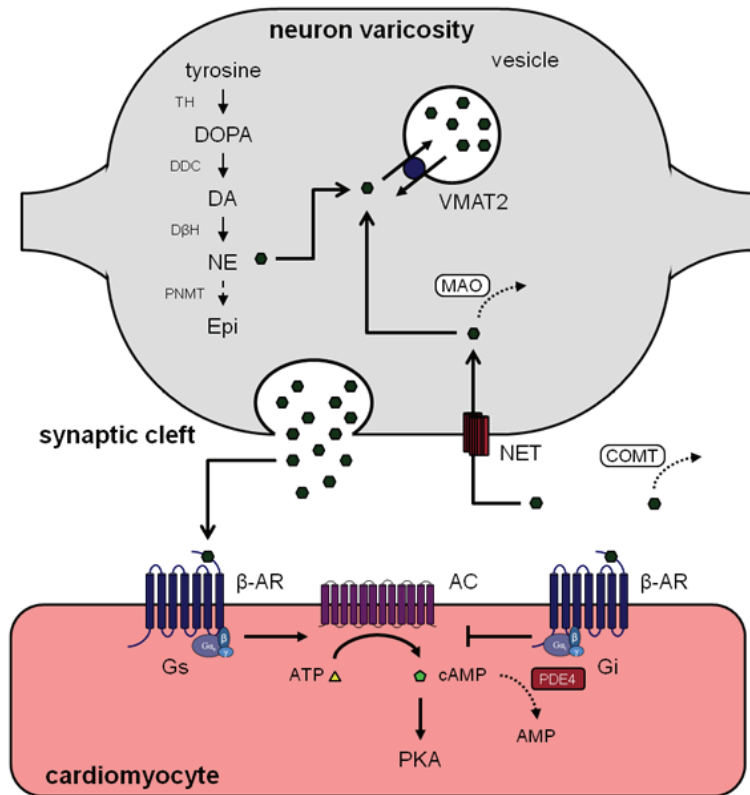
Figure 1. Noradrenergic neuroeffector junction. Norepinephrine (NE) is released into the synaptic cleft where it is bound to postsynaptic β-adrenoceptors (β-AR). Stimulation of G_s-coupled β-AR activate adenylate cyclase (AC) production of cAMP and downstream activation of protein kinase A (PKA). cAMP is broken down by phosphordiesterase-4 (PDE4). NE is recovered to the varicosity by NE reuptake transporter (NET). Abbreviations: TH, tyrosine hydroxylase; DOPA, dihydroxyphenylalanine; DDC, dopamine decarboxylase; DA, dopamine; DβH, dopamine β-hydroxylase; PNMT, phenetanolamine-*N*-methyltransferase; Epi, epinephrine; VMAT2, vesicular monoamine transporter-2; MAO, monoamine oxidase; COMT, catechol-O-methyltransferase.

nephrine concentration is localized to the sinoatrial node, atrioventricular node, and atria as compared to the ventricles [2]. Sympathetic stimulation of the conduction system produces elevated heart rate.

Activation of sympathetic neurons evokes release of the neurotransmitter norepinephrine into the synaptic cleft where it binds to G protein-coupled adrenoceptors at the cardiomyocyte membrane [3] (**Figure 1**). β-Adrenoceptors are positively coupled to stimulatory G protein $G\alpha_s$, which activates the cAMP/PKA signaling cascade, culminating in enhanced Ca^{2+} influx and cardiac contractility [4]. The $β_2$- and $β_3$-adrenoceptor isoforms are also coupled to inhibitory G protein $G\alpha_i$, which reduces cAMP production providing balance in noradrenergic signaling [3].

The sympathetic signal is terminated by active recapture of the neurotransmitter into the neuronal varicosity by the sodium-dependent norepinephrine reuptake transporter (NET) via the uptake-1 pathway [5, 6]. Norepinephrine is further packaged into neuronal vesicles by vesicular monoamine transporter-2 (VMAT2) [7, 8] or metabolized by monoamineoxidase (MAO) and catechol-*O*-methyltransferase

extrinsic control of heart rate and contractility. Sympathetic projections from the central nervous system synapse at the stellate and thoracic ganglia, where postganglionic fibres project to the heart [1, 2]. A complex network of sympathetic neurons innervates the epicardium, with a homogeneous distribution of fibres to the entire heart. Localized varicosities (boutons) along the length of the terminal axon act as storage and release points of norepinephrine forming relatively dispersed synapses compared to central nervous system junctions [1]. Regional tissue concentrations of norepinephrine are considered the gold standard measurement of cardiac sympathetic activation. The highest norepi-

(COMT) [9].

Diabetic heart

Metabolic and contractile adaptation

The complex changes in metabolic and contractile cardiac function in the progression of diabetes have been extensively reviewed [10, 11]. Briefly, the diabetic heart exhibits a shift in metabolic substrate preference to almost exclusive utilization of fatty acids over glucose [12, 13]. This shift exacerbates insulin resistance [14, 15] and contributes to the accumulation of lipid metabolites [16, 17] and advanced glyca-

tion end products [18, 19], leading to oxidative stress and myocardial fibrosis. These structural and metabolic changes culminate in the deterioration of contractile function, manifesting initially as reduced ventricular compliance and abnormal diastolic function, progressing to mild systolic impairment [20, 21]. To compensate for failing systolic function, the SNS may be activated.

Circulating factors

In addition to the compensatory activation, elevated plasma concentration of several factors have been shown to augment SNS activity. Elevated endogenous or exogenous glucose produces elevated circulating levels of norepinephrine [22-24]. Similarly, hyperinsulinemia has been linked to increased SNS activity [25, 26]. Administration of exogenous fatty acids enhances muscle sympathetic nerve activity by 45%, with resultant increases in heart rate and blood pressure [27].

Diabetic cardiac autonomic neuropathy

Diabetic autonomic neuropathy is a late stage complication of prolonged diabetes characterized by the development of neuroaxonal dystrophy, a swelling of distal neuronal axons without relative neuron loss [28]. Whereas early diabetes has been associated with elevated sympathetic tone, autonomic neuropathy results in a decrease in cardiac norepinephrine content and an accumulation of neurotrophins consistent with damage sustained by sympathetic neurons [29, 30]. Accumulation of advanced glycation end products, activation of apoptotic signals, oxidative stress, and elevated basal firing rate contribute to the degeneration of sympathetic neurons [31, 32].

SNS in diabetes

The presence of abnormal SNS signaling in the diabetic heart has been well established, as evidenced by direct and indirect measurements. It is unclear as to the order of sympathetic hyperactivity and development of insulin resistance, with some investigators purporting that insulin resistance is precipitated by a primary increase in sympathetic tone [33, 34], and others claiming independent development of insulin resistance and hyperinsulinemia promoting sympathetic drive [35]. Because of the complex interaction of SNS activity, hyperglycemia, hyperinsulinemia, metabolism, and insulin resistance it is difficult to define the primary insult. Recent clinical evaluations have attempted to define a temporal progression from sympathoadrenal activation to insulin resistance. A recent meta-analysis has suggested that SNS dysfunction is present in 51.9% of diabetic patients, but is likely underestimated due to reliance on somewhat crude tests [36].

Norepinephrine measurements

Elevated norepinephrine turnover and accumulation of neuronal norepinephrine have been found in diabetic animal models. Ganguly and colleagues demonstrated a twofold increase in cardiac and plasma norepinephrine concentration after 8 weeks of diabetes induced by streptozotocin (STZ) in rats [23]. Studies in isolated perfused diabetic hearts revealed enhanced catecholamine turnover, evidenced by elevated tyramine-induced norepinephrine release, increased initial rate of uptake of ^{3}H-norepinephrine, and reduced half time of ^{3}H-norepinephrine turnover. These parameters were normalized by treatment with insulin at 4 weeks after diabetes induction [23, 37]. Elevated norepinephrine levels have been described in a number of animal models and durations of diabetes, including STZ-induced type 1 diabetes [38], insulin-resistant intraperitoneal STZ-induced diabetes [24, 39], Zucker Diabetic Fatty rats [40], and non-obese Goto-Kakizaki type 2 diabetic rats [41].

These findings are supported by histofluorescence studies using glyoxylic acid, demonstrating increased fluorescent noradrenergic varicosities after 1 month of STZ-induced diabetes. In the same study, high performance liquid chromatography-quantified ventricular norepinephrine levels were elevated by 48-58% in 1 month diabetics compared to controls [42]. At 4 weeks of diabetes, STZ rats show reduced dopamine content in stellate ganglia, but an increase of ventricular norepinephrine, suggesting enhanced local conversion of neurotransmitter. No change in brain or plasma norepinephrine content was observed at this time point [43].

Sympathetic nerve activity

Electrode measurement of renal sympathetic nerve activity showed a reduced ability to adapt

to volume expansion in STZ diabetic rats compared to controls, associated with a blunted change in heart rate following phenylephrine administration [44]. Splanchnic sympathetic nerve activity response to phenylephrine was dampened in obese adult Zucker rats compared to age-matched lean Zucker rats in the absence of overt diabetes [45].

Baroreceptor reflex

The baroreceptor reflex is an indirect indicator of SNS activation in the heart, reflecting responsiveness to α-adrenergic stimulation. Left aortic depressor nerve activity measurements taken in OVE26 transgenic type 1 diabetic mice demonstrated a reduction in baroreflex control of heart rate in response to phenylephrine or sodium nitroprusside [46]. Pressure transducer evaluation in type 1 diabetic rats at baseline compared to non-diabetic controls describe reduced mean arterial pressure (-12%), heart rate (-13%) and lower rates of isolvolumic pressure development and decay following phenylephrine challenge [47].

Heart rate variability

Advancement of implantable telemetry transducer/receiver technology has facilitated longitudinal analysis of sympathetic tone in diabetic rats. Power spectral analysis provides a surrogate measurement of baroreceptor reflex activity and the quantification of heart rate variability [48-51].

Heart rate variability (standard deviation of normal heart rhythm, SDNN) has been demonstrated to be reduced by 50% (18 vs 36 bpm) within days of diabetes induction by STZ compared to non-diabetic controls [52, 53]. Low frequency to high frequency power ratio progressively increased over time, suggesting declination of high frequency (parasympathetic) and mid frequency (sympathetic) density [53]. Treatment with insulin was insufficient to restore heart rate variability to control levels, though there was a a modest recovery of heart rate: 362 vs 266 vs 303 bpm in non-diabetic, diabetic, and insulin-treated diabetic rats, respectively [54].

In Goto-Kakizaki non-obese type 2 diabetic rats a less prominent but significant reduction of heart rate variability SDNN compared to non-

diabetic controls was observed at 2 months (-24%) and 7 months (-16%), but was attenuated at 15 months of age (-5%) [55]. This is consistent with reduced heart rate variability during aging [55], with parallel changes in NET expression and reuptake function reported [56]. The differences in heart rhythm derive in part from extended duration of electrocardiogram QRS complex with no difference in QT interval between groups [55]. Prolonged QRS is consistent with delayed repolarization as observed in STZ rats [57-59].

Continuous telemetric monitoring in db/db type 2 diabetic mice describes a blunting of baroreflex regulation of heart rate, calculated by sequence method and cross-spectral analysis. Whereas blockade of sympathetic signaling with metoprolol decreased heart rate substantively in db/db mice, the effect was negligible in db/+ mice, consistent with constitutive activation of the cardiac SNS [60]. Atropine blockade of parasympathetic tone was also blunted in db/db mice compared to db/+ controls [60]. Conversely, study of non-obese diabetic mice showed the presence of sympathetic neuropathy, evidenced by elevated baroreceptor reflex activity that was not attenuated by metoprolol administration [61]. Heart rate variability measurement demonstrated reduced standard deviation of R-R interval in db/db mice compared to db/+ controls [60].

Power spectrum density analysis of systolic arterial pressure in diabetic rats revealed a progressive reduction of intermediate frequency (0.25-0.65 Hz), the range generally corresponding to sympathetic modulation of vascular tone, remaining fairly consistent over 1 to 18 weeks after STZ induction of diabetes [62].

These findings have been replicated in the clinical population. A study of young Norwegian males demonstrated that those in the highest quartile elevation of plasma norepinephrine during cold pressor test showed elevation of fasting plasma glucose level and homeostasis model assessment of insulin resistance at 18-years follow-up. This observation suggests that early sympathetic dysfunction may partially underlie subsequent development of insulin resistance and pre-diabetes [63]. A similar result was obtained by heart rate variability analysis over 8 year follow up in the Atherosclerosis Risk in Communities (ARIC) trial. In this case, indi-

Table 1. β-Adrenoceptor Expression in Diabetic Heart

Diabetic Model	Duration	Measurement	Isoform(s)	B_{max}*	% Diff†	Ref
SD, alloxan 35 mg/kg iv	5 days	³H-DHA binding	all	47±4	-51%	[74]
SD, STZ 65 mg/kg ip	2 weeks	³H-DHA binding	all	35±4	-6%	[68]
		CGP20712 block, high affinity	$β_1AR$	10±1	-46%	
		CGP20712 block, low affinity	$β_2AR$	24±1	+37%	
WK, STZ 45 mg/kg iv	4-6 weeks	³H-CGP12177 binding	all	33±7	-51%	[72]
WK, STZ 60 mg/kg iv	6 weeks	Western immunoblotting	$β_1AR$		-65%	[77]
			$β_2AR$		+61%	
			$β_3AR$		+140%	
WK, STZ 55mg/kg iv	8 weeks	¹²⁵I- CYP binding	all	36±4	-31%	[73]
SHR, STZ 55 mg/kg iv	8 weeks	¹²⁵I- CYP binding	all	35±5	-34%	[73]
SD, STZ 45 mg/kg ip, high fat feeding	8 weeks	³H-CGP12177 *ex vivo* biodist.	all		-40%	[127]
		Western immunoblotting	$β_1AR$		-15%	
			$β_2AR$		+12%	
SD, STZ 65 mg/kg iv	10 weeks	³H-CGP12177 binding	all	92±4‡	-41%	[76]
WK, STZ 45 mg/kg iv	14 weeks	Western immunoblotting	$β_1AR$		-45%	[67]
			$β_2AR$		-17%	
			$β_3AR$		+200%	
SD, STZ 65 mg/kg iv	13 weeks 26 weeks	³H-DHA binding	all	28±3 23±2	-13% -21%	[75]

* fmol/mg protein; † (Diabetic – Control) / Control × 100%; ‡ fmol/10⁶ cells. SD, Sprague Dawley rat; WK, Wistar Kyoto rat; SHR, Spontaneously Hypertensive Rat; DHA, dihydroalprenolol; ¹²⁵I-CYP, ¹²⁵I-cyanopindolol; biodist, biodistribution

viduals falling in the lowest quartile of heart rate variability (either standard deviation of R-R interval or low-frequency power) were 60% more likely than the highest quartile to develop insulin resistance or diabetes [64]. It has been reasoned that sustained sympathetic activation may augment lipid metabolism, leading to elevated circulating fatty acids and insulin resistance [64].

β-Adrenoceptor expression

The persistent elevation of catecholamines evokes downregulation of cardiomyocyte β-adrenoceptors, and a shift in the isoform population to favour G_i-coupled $β_2$-adrenoceptors. This pattern is well characterized in the development of heart failure [65, 66], and has been extensively described in diabetes as well, including rats [67, 68], large animal models [69], and the patient population [70]. Reduced β-adrenoceptor expression has been consistently described in type 1 diabetic heart (**Table 1**), evidenced by significant reductions in total β-adrenoceptor binding in radioligand binding assays [67, 71-76].

Latifpour and McNeill established time depend-

ent changes in cardiac autonomic receptor expression patterns in type 1 diabetic STZ-treated rats [75]. At 3 months of diabetes compared to age-matched non-diabetic controls, only ³H-prazosin binding to α-adrenoceptors was reduced (B_{max} 66.6 vs 78.8 fmol/mg protein), with no difference in ³H-dihydroalprenolol or ³H-quinuclidinyl benzilate binding to β-adrenoceptors and muscarinic cholinergic receptors, respectively. By 6 months of untreated diabetes, binding to all three receptors was reduced by 21-28% (α-adrenoceptor: 56.4 vs 72.2; β-adrenoceptor: 22.5 vs 28.6; muscarinic: 84.8 vs 117.4 fmol/mg protein) [75].

Reduced β-adrenoceptor density in diabetes reflects a shift in relative expression of β-adrenoceptor subtypes as determined by Western immunoblotting [67]. Quantification of Coomassie staining showed a shift in $β_1$:$β_2$:$β_3$ expression profile from 62:30:8 in control to 40:36:23 in diabetic rat hearts [67]. This shift is similar to that observed during sympathetic hyperactivity in the development of heart failure [65]. In the same study, normalization of blood glucose by daily insulin injection for only 2 weeks following 12 weeks of chronic diabetes was sufficient to revert expression patterns to

normal, with a $\beta_1:\beta_2:\beta_3$ expression profile of 57:33:10 [67]. Displacement of ^{3}H-dihydroalprenolol by cold CGP20712 to distinguish high affinity β_1-adrenoceptor binding from low affinity β_2-adrenoceptor identified a shift in relative expression ($\beta_1:\beta_2$) from 52:48 in control to 30:70 in untreated diabetics, restored to 40:60 by insulin [68]. These findings establish the critical involvement of glycemia in the maintenance of β-adrenoceptor expression.

After 2.5 months of diabetes, internalization of β-adrenoceptors is evident, as determined by binding assays with the cell-surface impermeable ^{3}H-CGP12177 compared to lipophilic ^{125}I-iodocyanopindolol [76]. This observation suggests an increase in the internalization of β-adrenoceptors during diabetes, prior to overt degradation, which, in the context of other dihydroalprenolol studies, is suggested to occur by 6 months of diabetes. Treatment over 48 hours with insulin partially restored membrane surface ^{3}H-CGP12177 binding sites [76]. The rapid response to insulin suggests that early internalization and impairment of β-adrenoceptor signaling is readily reversible by glycemic control.

The altered expression patterns of myocardial β-adrenoceptors bear functional consequences. The reduced maximum rate of left ventricle dP/dt_{max} was associated with a reduction of isoproterenol-induced adenylate cyclase activity after 4 weeks of untreated diabetes, suggesting alteration of upstream signaling mediators [71]. Paradoxically, pressure transducer evaluation in type 1 diabetic rats following administration of low-dose β_1-adrenoceptor agonist dobutamine (1 µg/kg) showed nearly double maximal isovolumic pressure development and decay compared to controls. Insulin treatment normalized the response in diabetic rats. This suggests an increased sensitivity to β-adrenergic stimulation, consistent with an upregulation of β_1-adrenoceptors [47]. However, no attempt to quantify adrenoceptors was performed in this study.

In isolated perfused diabetic hearts (6 weeks post STZ), left ventricular developed pressure was significantly lower than controls by as much as 50% at higher left atrial filling pressure, associated with a 50% reduction in relative β_1-adrenoceptor expression [77]. Treatment with the β_1-adrenoceptor antagonist metoprolol not only increased expression of β-adrenoceptors in

diabetic hearts, but also improved mechanical performance in left ventricular pressures [77]. Sharma and colleagues further demonstrated concomitant improvement in metabolic performance in metoprolol-treated rats, characterized by an 80% increase in glucose oxidation, 39% decrease of palmitate oxidation, driven in part by a reduction in carnitine palmitoyl transferase-1B expression and activity [78, 79].

Downstream noradrenergic signaling

In addition to changes in innervation and receptors, downstream targets of the SNS have also been studied in diabetes. As early as 8 days after diabetes induction, the response of adenylate cyclase to β-adrenergic stimulation was ablated, whereas other pathways of adenylate cyclase activation remained intact [80]. No difference in dihydroalprenolol binding was observed [80], suggesting a functional uncoupling of adenylate cyclase from myocardial β-adrenoceptors. Additional evidence suggests that adenylate cyclase and cAMP inotropic effects are independently impaired in diabetes, with reduced contractile force observed in isolated perfused hearts following stimulation with adenylate cyclase activator forskolin, exogenous dibutyryl cAMP, or 3-isobutyl-1-methylxanthine (IBMX) [81]. Reduced expression of β-adrenoceptors in isolated perfused 4 week diabetic heart also affects calcium mobilization, wherein diabetic rats exhibit lower intracellular Ca^{2+} following stimulation with isoproterenol [82]. This anomaly would impair the contractile response to sympathetic stimulation and stress.

SNS imaging targets with PET and SPECT

Tracer-based imaging of the SNS has gained traction in recent years, progressing toward more mainstream clinical application. Targets of molecular imaging include evaluation of neuron integrity at the NET and evaluation of postsynaptic expression of β-adrenoceptors at the cardiomyocyte membrane (reviewed in [9, 83]) (**Figure 2A**). Additional autonomic targets include muscarinic receptors [84], angiotensin II type 1 receptors [85, 86] and intracellular signaling elements phosphodiesterase-4 [87] and diacylglycerol [88], though the validation of these tracers is at present unclear [89]. The bulk of SNS imaging has been focused on presynaptic measurements of reuptake function and postsynaptic adrenoceptor density.
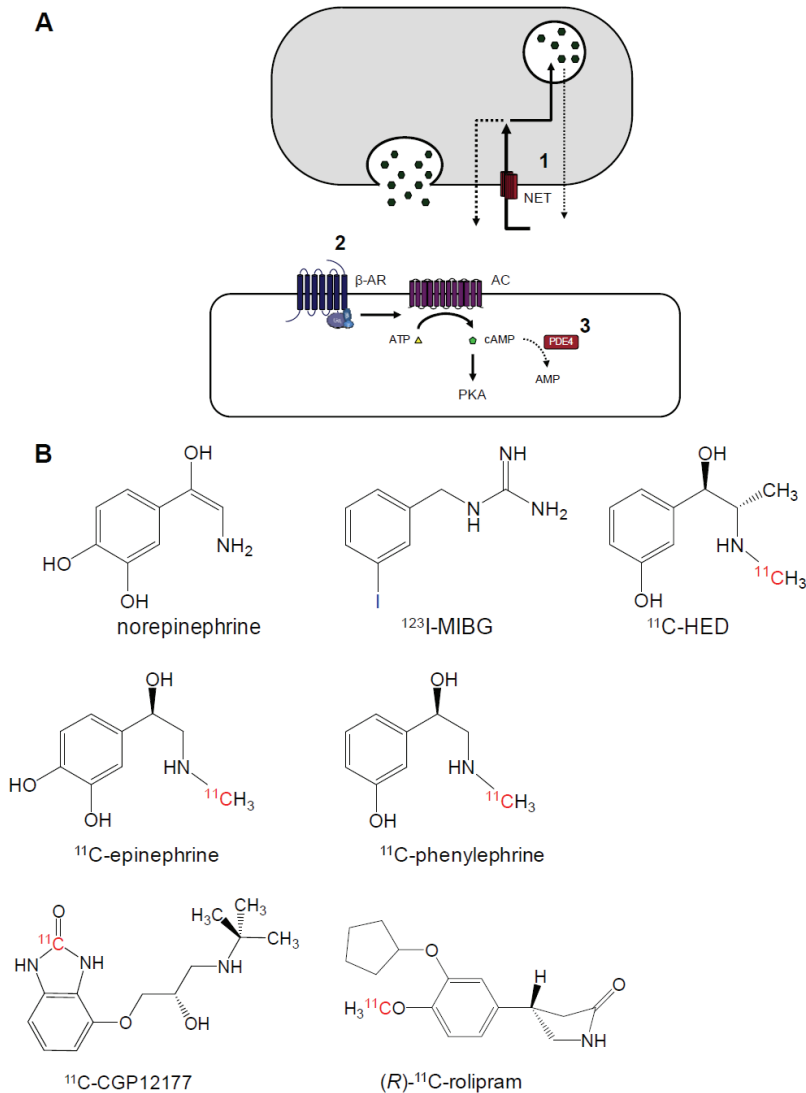
Figure 2. Established probes for evaluation of cardiac SNS. (A) Targets for molecular imaging in the sympathetic signaling include (1) presynaptic nervous integrity at NET; (2) postsynaptic β-AR density; and (3) indirect evaluation of cAMP levels and PKA activation at PDE4. (B) Chemical structures of probes for neurohormonal interrogation.

Neuronal imaging agents are generally analogues of norepinephrine (**Figure 2B**), that are taken up via the sodium-dependent NET (uptake-1) pathway. In SPECT, the prevalent tracer is radio-iodinated metaiodobenzylguanidine (^{123}I-MIBG). Availability and regulation has limited ^{123}I-MIBG use to research purposes, but recent advances have revealed an added-value of neuronal imaging using ^{123}I-MIBG among heart failure patients, which may accelerate its application as a clinical diagnostic tool

[90, 91]. In PET, ^{11}C-*meta*-hydroxyephedrine (^{11}C-HED), ^{11}C-phenylephrine, and ^{11}C-epinephrine have been evaluated with varying degrees of success (reviewed in [9, 92]). The development, characterization, and application of these radiotracers have been extensively studied and reviewed [9, 92, 93].

^{123}I-MIBG SPECT imaging

Briefly, retention of ^{123}I-MIBG was shown to be reduced by blockade of NET (uptake-1) [94] and following sympathectomy by phenol application in the canine heart [95], though a high degree of extraneuronal uptake (via uptake-2) is consistently observed in many animal species. Heart transplant recipients reflect this observation, with a complete lack of early and late ^{123}I-MIBG uptake by myocardium devoid of sympathetic innervation [9]. ^{123}I-MIBG has been applied in nuclear cardiology to examine post-myocardial infarct healing [96, 97], arrhythmia [98, 99], and progression of congestive heart failure [100]. Reduced contrast between the heart and the mediastinum is characteristic of impaired neuronal function, which also manifests as enhanced late tracer washout [90, 98, 101].

^{11}C-HED PET imaging

Advantages of the PET tracer ^{11}C-HED include high neuronal compared to extraneuronal uptake [102], long neuronal retention time due to partial packaging in vesicles [103], and metabolic stability due to resistance to catecholamine metabolism by MAO or COMT [104]. Due
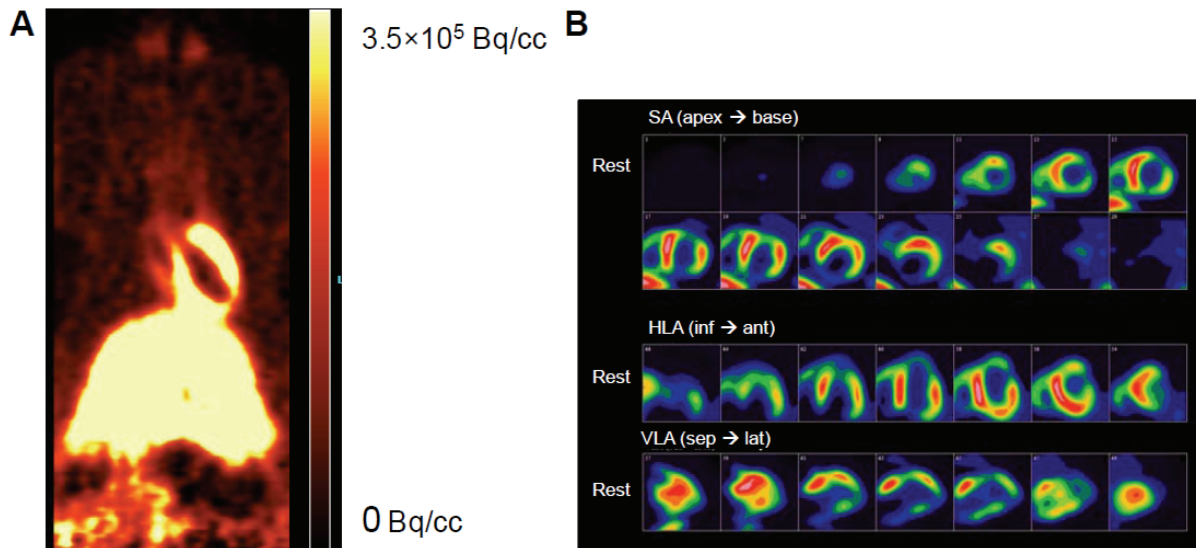
Figure 3. Sample ^{11}C-HED myocardial images. (A) Rat ^{11}C-HED coronal image obtained using Siemens Inveon DPET small animal camera showing heart and liver uptake. (B) Reoriented ^{11}C-HED PET cardiac image from a patient with obstructive sleep apnea obtained using GE Discovery D690 PET/VCT 64 camera.

to its lipophilicity, ^{11}C-HED can passively diffuse from the neuronal varicosity, and is also subject to active release during signal transduction. Kinetic studies have demonstrated the dependence of ^{11}C-HED retention on the availability of NET, established as susceptibility to blockade or displacement by the NET inhibitor desipramine. This has been observed in isolated perfused rat heart [94], *ex vivo* biodistribution in rats [105-107] and dogs [94, 108] and more recently using small animal PET in rats [93] and mice [109]. Retention of ^{11}C-HED is also subject to competition for limited reuptake sites with endogenous and exogenous neurotransmitter, as demonstrated by treatments with the precursor and false neurotransmitter metaraminol [107, 109], treatments to enhance endogenous norepinephrine such as tranylcypromine [105] and by infusion of exogenous norepinephrine [105]. Clinical applications of ^{11}C-HED have included post-infarct neuronal remodeling [110], tracking of post-transplant reinnervation [111, 112], arrhythmia [113, 114], congestive heart failure [115-117], hibernating myocardium [118, 119], hypertrophic cardiomyopathy [120], and coronary artery disease [121]. Evaluation of ^{11}C-HED in rats (**Figure 3A**) has demonstrated similar image quality to clinical images (**Figure 3B**), though accelerated tracer washout due to heightened basal sympathetic tone is observed in rats compared to humans [93].

[11]C-Phenylephrine is subject to metabolism by MAO to ^{11}C-methylamine, complicating kinetic modeling [93, 122]. ^{11}C-Epinephrine holds promise as a sympathetic neuronal marker with the added complication of labeled metabolites [93, 123]. Retention properties of both of these tracers are similar to ^{11}C-HED, with advantageous and disadvantageous characteristics (reviewed in [9]). Effectively, retention of ^{123}I-MIBG or ^{11}C-HED provides a dynamic semi-quantitative measurement of reuptake, storage, and release of norepinephrine from myocardial sympathetic neuronal varicosities.

[11]C-CGP12177 PET imaging

Non-invasive determination of β-adrenoceptor density is another target of interest in imaging the cardiac SNS. The bulk of research has been conducted using the non-selective ^{11}C-CGP12177 and its derivatives (**Figure 2B**). Labeled with tritium, CGP12177 has been utilized in binding assays to determine β-adrenoceptor density ex vivo [124, 125]. As a radiotracer, CGP12177 shows high and sustained uptake in myocardium compared to surrounding tissues in rat hearts, and is selectively blocked up to 90% by β-blockers propranolol, atenolol and unlabeled compound [126, 127]. Complicated synthesis has limited the use of ^{11}C-CGP12177 to some extent, though some clinical applications
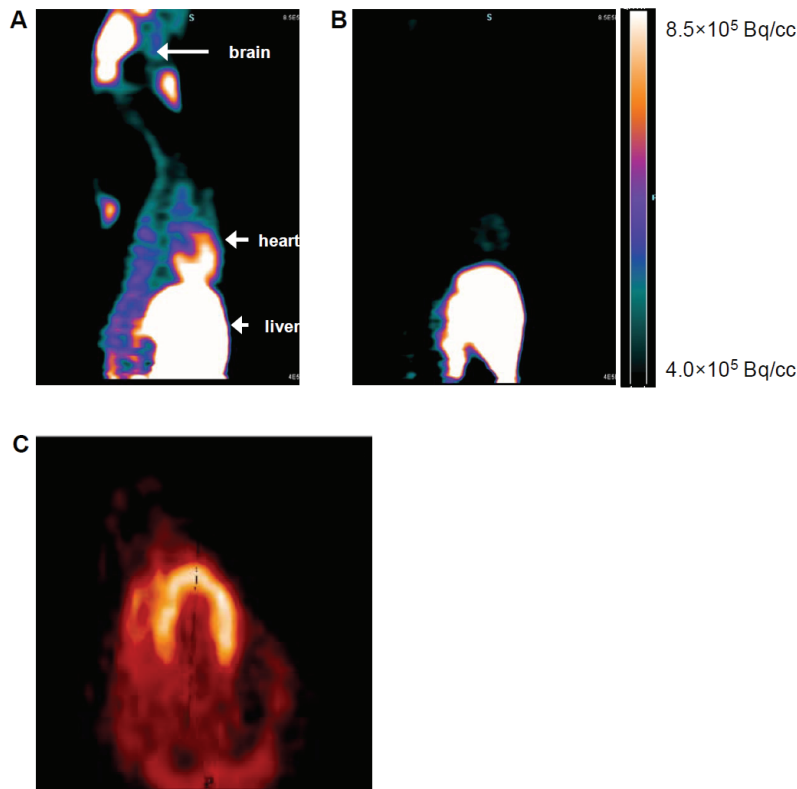
Figure 4. Sample (R)-^{11}C-rolipram images. (A) Rat (R)-^{11}C-rolipram sagittal whole body image obtained using Siemens Inveon DPET small animal camera showing heart, brain, and liver uptake. (B) Coinjection of cold (R)-rolipram blocks the specific binding of (R)-^{11}C-rolipram to phosphodiesterase-4 in brain and heart. (C) Summed canine (R)-^{11}C-rolipram coronal image obtained using ECAT-ART cardiac PET camera shows myocardial uptake.

been limited to preclinical evaluations, but ex vivo biodistribution studies suggest that CGP12177 is a suitable radiotracer for longitudinal evaluation of β-adrenoceptor density in the diabetic heart [127].

(R)-^{11}C-Rolipram PET imaging

(R)-^{11}C-Rolipram (**Figure 2B**) has been characterized in small animals for evaluation of phosphodiesterase-4 expression in the heart, providing an indirect index of intracellular cAMP activation. Preliminary evaluation of (R)-^{11}C-rolipram imaging has illustrated quality myocardium-to-blood and myocardium-to-background contrast and specific binding in rats (**Figure 4AB**) and dogs (**Figure 4C**) [132, 133]. Cardiac binding of (R)-^{11}C-rolipram was enhanced by treatments elevating endogenous norepinephrine and reduced when phosphodiesterase-4 is blocked [133, 134]. By contrast in animal models of chronic obesity and acute adriamycin-induced cardiotoxicity, characterized by elevated sympathetic drive and catecholamine levels, no increase in (R)-^{11}C-rolipram cardiac binding was observed in response to blockade of the NET by desipramine and increased synaptic norepinephrine [135, 136]. This finding is consistent with downregulation of β-adrenoceptors.

have emerged, including use in post-myocardial infarction [128], heart failure [117, 129], hibernating myocardium [119], and non-ischemic cardiomyopathy [130, 131]. A correlation has been described between pre- and post-synaptic function, as assessed with ^{11}C-HED and ^{11}C-CGP12177, respectively, with similar reduction in sympathetic neuron integrity and myocardial β-adrenoceptor density observed among subjects with congestive heart failure [116, 129]. A similar correlation was described to early and delayed late heart-to-mediastinal ratio of ^{123}I-MIBG [131]. In a small scale trial in patients with stable chronic heart failure due to idiopathic cardiomyopathy, β-adrenoceptor density measured by ^{11}C-CGP12177 PET predicted 20 month response to carvedilol treatment, wherein the patients with the lowest CGP12177 binding showed the greatest improvement in left ventricular ejection fraction [130]. Application of CGP12177 in the diabetic heart has

Preclinical imaging of SNS in diabetes

The development of specific radiotracers and dedicated small animal imaging systems has facilitated the interrogation of cardiac sympathetic nervous integrity in rodent models of diabetes using SPECT and PET imaging, ex vivo biodistribution, and autoradiography techniques (**Table 2**).

^{123}I-MIBG preclinical imaging in diabetes

A small number of preliminary imaging studies have been conducted using radioiodinated ^{123}I-

Table 2. Summary of Preclinical Myocardial Presynaptic Imaging Studies in Diabetic Rodents

Model	Duration	Tracer	Method	Finding	Ref
SD, STZ 55 mg/kg iv	4 weeks	^{125}I-MIBG	*ex vivo* autoradiography	-13% inferior LV retention	[140]
SD, STZ 45 mg/kg ip, high fat feeding	8 weeks	^{11}C-HED	*ex vivo* biodistribution	-12% LV retention	[24]
WK, STZ 50 mg/kg ip	6 months 9 months	^{11}C-HED	*ex vivo* biodistribution	-33% distal LV retention -40% proximal LV retention -44% distal LV retention	[30]
Goto Kakizaki	8 weeks	^{125}I-MIBG	*ex vivo* autoradiography	-23% anterior LV retention -41% inferior LV retention	[41]
WK, STZ 60 mg/kg iv	8 weeks	^{123}I-MIBG	pinhole SPECT	-58% counts x kg / pixel +61% washout rate	[139]
SHR, STZ 60 mg/kg	8 weeks	^{123}I-MIBG	pinhole SPECT	-58% counts x kg / pixel +34% washout rate	[139]
Zucker Obese	22 weeks	^{123}I-MIBG	pinhole SPECT	+272% counts x kg / pixel +44% washout rate	[139]
WK, STZ 60 mg/kg iv	8 weeks	^{123}I-MIBG	small animal SPECT	+64% washout rate	[138]
mice, STZ 35 mg/kg ip × 5 d	7 months	^{123}I-MIBG	small animal SPECT	+95% LV washout rate +14% initial LV uptake	[137]

SD, Sprague Dawley; WK, Wistar Kyoto; SHR, Spontaneously Hypertensive Rat; ^{123}I-MIBG, metaiodobenzylguanidine; ^{11}C-HED, hydroxyephedrine

MIBG in diabetic rodents. Small animal SPECT imaging revealed maintained uptake but enhanced myocardial washout of ^{123}I-MIBG over 30-120 min after injection among STZ diabetic C57/Bl6 mice compared to controls (41 vs 21%). Liver washout and urinary excretion were also accelerated. ^{3}H-Desipramine binding assay demonstrated a reduction of NET density (B_{max}) in hearts of diabetic compared to non-diabetic mice (136 vs 244 fmol/mg protein) with no change in binding affinity (k_d) [137]. Maintained initial uptake with enhanced washout suggests the presence of functional sympathetic nerve terminals and elevated sympathetic tone, with downregulation of NET consistent with other models of diabetes [24, 41].

Similar observations were made using pinhole SPECT studies in Wistar STZ rats, with washout acceleration to 21.0 as compared to 12.8 %/h in non-diabetic controls [138]. Evaluation of ^{123}I-MIBG in STZ rats at 8 weeks demonstrated reduced uptake at 60 min after injection compared to age-matched healthy controls and accelerated washout over 4 hours (36 vs 22%). The altered tracer kinetics were corroborated by an elevation of plasma norepinephrine (3.6 vs 2.4 nmol/l) and reduced β-adrenoceptor expression measured by ^{125}I-cyanopindolol binding assay (36 vs 52 fmol/mg protein) [139]. In comparing Zucker obese with lean rats at 22 weeks

of age, obese animals displayed higher initial uptake of ^{123}I-MIBG (0.67 vs 0.18 counts × kg body weight / pixel × injected dose). However, the washout was significantly accelerated in obese compared to lean rats (44 vs 19%) [139]. No change in norepinephrine was observed, but β-adrenoceptor density was 15% lower in Zucker obese rats.

In ex vivo studies, regional distribution of ^{125}I-MIBG was compared with sestamibi (MIBI) using autoradiographic techniques in STZ diabetic rats to discern sympathetic neuronal density and perfusion, respectively. A decrease in inferior wall ^{125}I-MIBG distribution absorption ratio was observed in 10 week diabetic rats, with no comparable decrease observed in MIBI distribution. By contrast, no difference was reported in control rats. These observations correlated to an increase in regional norepinephrine levels in diabetic compared to non-diabetic rats (8.2 vs 4.3 µg/g anterior wall; 8.7 vs 3.9 µg/g inferior wall) and a moderate decrease in inferior wall NET density (641 vs 809 fmol/mg protein) as measured by ^{3}H-desipramine binding assay [140]. This suggests that while blood flow was maintained, a regional impairment of anterior sympathetic innervation was apparent. In non-obese type 2 diabetic Goto-Kakizaki rats (8 weeks old), the same investigators described maintained MIBI and a moderate decrease in

^{125}I-MIBG inferior to anterior wall distribution absorption ratio. No difference in regional cardiac norepinephrine concentration was detected between Goto-Kakizaki and non-diabetic rats, but a dramatic reduction of NET density was observed by binding assay (263 vs 364 fmol/mg protein anterior wall; 251 vs 459 fmol/mg protein inferior wall) [41].

11C-HED preclinical imaging in diabetes

Distribution of ^{11}C-HED has been assessed in STZ-induced diabetic rats using gamma counting techniques. At 6 months of diabetes, STZ rats exhibited a significant 33% reduction of ^{11}C-HED retention restricted to the distal left ventricle compared to non-diabetic controls, with a mild but significant increase in left ventricle norepinephrine (711 vs 600 ng/g proximal; 613 vs 491 ng/g distal). By 9 months of diabetes, this defect was observed in the entire left ventricle, with reduced HED accumulation by 40-44% in proximal and distal left ventricle segments. At the 9 month timepoint, significant reduction of norepinephrine (503 vs 694 ng/g proximal; 351 vs 536 ng/g distal) and nerve growth factor (4.1 vs 10.1 ng/g proximal; 2.9 vs 7.4 ng/g distal) was described. Taken together these data indicated that while autonomic neuropathy was present at 9 months, this was preceded (at 6 months) by a regional dysregulation of sympathetic neurons during which norepinephrine release was not impeded [30].

A similar result was obtained at 2 months of diabetes in STZ diabetic rats fed high fat diet to produce insulin resistance. Retention of ^{11}C-HED in cardiac regions was globally reduced by 15-30%, with a corresponding increase in cardiac norepinephrine levels (20%) and a decrease in NET expression (-17%) compared to age-matched, high fat diet-fed controls. Immunostaining for tyrosine hydroxylase confirmed the maintenance of intact sympathetic neurons in the left ventricle of diabetic rats [24]. Collectively, these studies have built a foundation for further longitudinal evaluation of sympathetic dysregulation in the diabetic rodent heart.

Postsynaptic preclinical imaging in diabetes

To date, no small animal imaging has been conducted using ^{11}C-CGP12177 derivatives to visualize cardiac β-adrenoceptors. In high fat diet-fed STZ diabetic rats, 8 weeks of hyperglycemia was shown to reduce specific binding of ^{3}H-CGP12177 to cardiac β-adrenoceptors by 30-40% compared to controls [127]. This result was in conjunction with a significant decrease in relative myocardial β_1-adrenoceptor expression and no change in relative β_2-adrenoceptor expression compared to controls [127], consistent with receptor internalization and degradation following sustained hyperglycemia. Norepinephrine levels in hyperglycemic rats were elevated 2.5 fold in plasma and 1.2 fold in myocardium [24]. This study supports the suitability of ^{11}C-CGP12177 for longitudinal study of membrane β-adrenoceptor expression during the development and treatment of diabetes.

The evidence of altered adenylate cyclase regulation [80] suggests a potential role for the phosphodiesterase-4 inhibitor (R)-^{11}C-rolipram as a surrogate marker of cAMP activity during the development of diabetic cardiomyopathy. In conditions of sympathetic hyperactivity such as diabetes, examination of myocardial phosphodiesterase-4 expression and activity may provide insight into the development of signaling abnormalities.

Clinical imaging of SNS in diabetes

123I-MIBG clinical imaging in diabetes

SNS imaging studies in the diabetic patient population have largely been limited to investigation of presynaptic nervous integrity using ^{123}I-MIBG SPECT or ^{11}C-HED PET. Evaluation of post-synaptic β-adrenoceptors in human subjects has been limited. The trials have overwhelmingly focused on type 1 diabetes and the development of autonomic neuropathy, though some instances of early sympathetic dysregulation in diabetes have also been described (**Table 3**).

Mean late heart-to-mediastinal ratio of ^{123}I-MIBG uptake was significantly lower in diabetic subjects compared to non-diabetic subjects, regardless of heart failure progression. Among diabetic patients, lower heart-to-mediastinal ^{123}I-MIBG late uptake ratio (<1.60) was associated with three times greater rate of heart failure progression as compared to diabetic patients with a normal (>1.60) heart-to-mediastinal ^{123}I-MIBG uptake ratio (33.5 vs 11.2% event rate) [141]. There was no difference in plasma norepinephrine levels between diabetic and non-diabetic subjects, suggesting greater prognostic

Table 3. Summary of Clinical Myocardial Presynaptic Imaging Studies in Diabetic Patients

Tracer	N	Groups	Finding	Ref
[11]C-HED	10	type 1 diabetic	- reduced retention index (-30%) in diabetics	[144]
	11	healthy controls	- increased retention index (+25%) 3 y follow-up, good control	
			- decreased retention index (-14%) 3 y follow-up, poor control	
[11]C-HED	16	diabetic MNA	- increased area of retention defects (36% of LV) in MNA patients	[147]
	12	diabetic	compared to diabetic controls (<1% of LV)	
	10	non-diabetic		
[11]C-HED	23	CAD	- slightly lower retention (-2.5%, p=0.0007) at 1 y follow up in	[146]
	10	type 2 diabetic	diabetic CAD patients	
	13	non-diabetic	- no change in non-diabetic CAD patients at 1 y	
^{123}I-MIBG	11	diabetic	- reduced 1-y follow-up uptake score in poor glucose control	[145]
			- no change 1 y follow-up ^{123}I-MIBG uptake in good glucose control	
^{123}I-MIBG	7	CAN	- reduced H/M ratio in CAN patients	[143]
	26	healthy controls	- correlation of H/M ratio to early diastolic tissue velocity (r^2=0.32, p=0.01)	
^{123}I-MIBG	33	type 2 diabetic	- enhanced washout in hypertensive diabetic (+20%)	[142]
	15	hypertensive	- lower H/M ratio in hypertensive diabetic (-14%)	
	18	normotensive		
^{123}I-MIBG	961	NYHA II-III	- lower H/M ratio in diabetics vs non-diabetics	[141]
	343	diabetic	- lower H/M ratio in diabetics with heart failure progression	
	618	non-diabetic		

MNA, microangiopathy; CAD, coronary artery disease; CAN, cardiac autonomic neuropathy; H/M heart-to-mediastinal ratio

power from neuronal imaging.

Greater impairment in baroreflex sensitivity was found among hypertensive type 2 diabetic patients as compared to normotensive diabetics, paralleled by a modest decrease in ^{123}I-MIBG uptake (heart-to-mediastinum ratio) at early and delayed stages and an increased washout rate [142]. No difference in high and low frequency power heart rate variability or plasma norepinephrine was found between these subgroups of diabetics [142].

In a study of 114 patients, autonomic function testing by heart rate variability and reflex tests identified 16 patients with cardiac autonomic neuropathy. Patients with neuropathy exhibited a modest decrease in ^{123}I-MIBG heart to mediastinal ratio compared to those without (1.6 vs 1.8) which significantly correlated with reduced resting tissue Doppler peak early diastolic velocity (4.7 vs 6.3 cm/s) [143]. Regional analysis demonstrated denervation particularly localized to the anterior and lateral walls of the ventricle [143].

[11]C-HED clinical imaging in diabetes

Stevens and colleagues described a defect in ^{11}C-HED retention in ~7-9% of the distal left ventricle of diabetic patients, consistent with

sympathetic denervation or dysinnervation [144]. At 3 years follow up, among patients who subsequently achieved good glycemic control this deficit of ^{11}C-HED retention index was reduced by 77% compared to the first scan, and average retention index score in proximal and distal segments improved by 30%. By contrast, among patients with poor glycemic control the size of the apical defect was increased by 340%, with distal segments showing a further 21% decrease in retention index [144]. Interestingly, no improvement in autonomic reflex test scores was observed among the patients with good glycemic control [144]. A similar capacity for recovery was shown in a 1 year follow-up scintigraphy study among type 1 diabetic patients, wherein patients achieving glycosylated hemoglobin <8% exhibited significant reduction of global and regional ^{123}I-MIBG uptake score [145].

In the presence of coronary artery disease, fixed defects of ^{11}C-HED retention remain, but were not complicated by the presence of diabetes. The defect size of ^{11}C-HED did not increase in size or severity over a 1 year follow up among coronary artery disease patients during normal therapy [146]. These patients exhibited good glucose control, with HbA1c levels of 6.9±0.9%, matching the cutoff value for glycemic control previously identified [144]. However, in seg-

ments with severely reduced coronary flow reserve, a significant reduction of ^{11}C-HED retention was observed, which was purported to reflect ischemic rather than hyperglycemic neuronal damage [146].

Indeed, in a small cohort Pop-Busui and colleagues identified a significant difference in ^{11}C-HED retention as affected area among type 1 diabetic patients with early microangiopathy as compared to the stable patient population. Diabetic patients showed generally lower plasma norepinephrine levels at rest, an amplified response to the cold pressor test, baroceptor reflex impairment, and echocardiographic indicators of diastolic dysfunction [147]. In addition, myocardial blood flow reserve was reduced in diabetics compared to healthy subjects, and reduced further in the diabetic group with early microangiopathy [147]. This loss of flow reserve may derive from loss of vascular response to norepinephrine stimulation, consistent with constitutively hyperactivated sympathetic nervous drive. Together, these observations support the presence of abnormal noradrenergic signaling and presynaptic sympathetic function even in the absence of diabetic autonomic neuropathy.

Recent clinical investigations with ^{123}I-MIBG have made a strong case for the prognostic value of molecular imaging of the cardiac SNS. Heart-to-mediastinal uptake ratio of ^{123}I-MIBG (<1.60 threshold) was independently predictive of heart failure progression, arrhythmic events, cardiac death, and all-cause mortality among a heart failure patient population over a two year period [90]. While this study did not directly evaluate the benefit of ^{123}I-MIBG imaging in these patients, it provides a solid foundation for the use of sympathetic imaging data in the stratification of patient risk to inform long term treatment options. Subjects with events had a modest elevation of plasma norepinephrine compared with event-free subjects (722 vs 642 pg/ml), but norepinephrine levels alone were not of prognostic value in the study [90]. In previous reports, plasma norepinephrine has been identified as an independent predictor of cardiac events in heart failure patients [148].

Collectively, the clinical data strongly support the utility of ^{123}I-MIBG SPECT and ^{11}C-HED PET imaging in stratifying risk of cardiovascular events among diabetic patients, particularly progression to heart failure and sudden cardiac

death. The regression of sympathetic defects to glycemic control underscores the relationship between hyperglycemia, norepinephrine, and cardiac noradrenergic signaling, and suggests that altered regulation of sympathetic neuronal signaling precedes overt neuropathy.

Future perspectives

Considerable evidence from basic and clinical studies have established the presence of abnormal SNS signaling in the diabetic heart, as both a consequence and cause of systolic and diastolic dysfunction. Diabetes evokes elevated systemic and cardiac norepinephrine, leading to blunted baroreceptor adrenergic reflex, reduced heart rate variability, and downregulation of signaling elements including presynaptic NET and postsynaptic β-adrenoceptors (**Figure 5**). These abnormalities partially underlie the added risk of cardiovascular morbidity and mortality incurred by the diabetic population. As molecular imaging research in this area progresses, a number of opportunities and questions stand to be addressed.

As discussed in this review, the bulk of present studies have focused on the development of sympathetic neuronal changes in type 1 diabetes, with limited imaging and non-imaging evaluation in the type 2 diabetic population. Preclinical imaging studies in established models of type 2 diabetes may provide additional insight into the progression of autonomic neuropathy and sympathetic signaling abnormalities in the development of diabetes. Some evidence suggests that neuropathy is either delayed or absent in this population, providing the opportunity to study sympathetic hyperactivity and increased myocardial norepinephrine release and the effects of therapies to dampen this sympathetic signal.

The continued development of micro imaging techniques will permit a longitudinal assessment of diabetes progression in small animal models. Basic research suggests that denervation is preceded by a transient period of sympathetic hyperactivity, which may contribute to the deterioration of myocardial performance. Serial studies in diabetic animals would facilitate the complementary analysis of sympathetic neuronal imaging, functional measures such as echocardiography and left ventricular hemodynamics, and in vitro determination of pathologi-
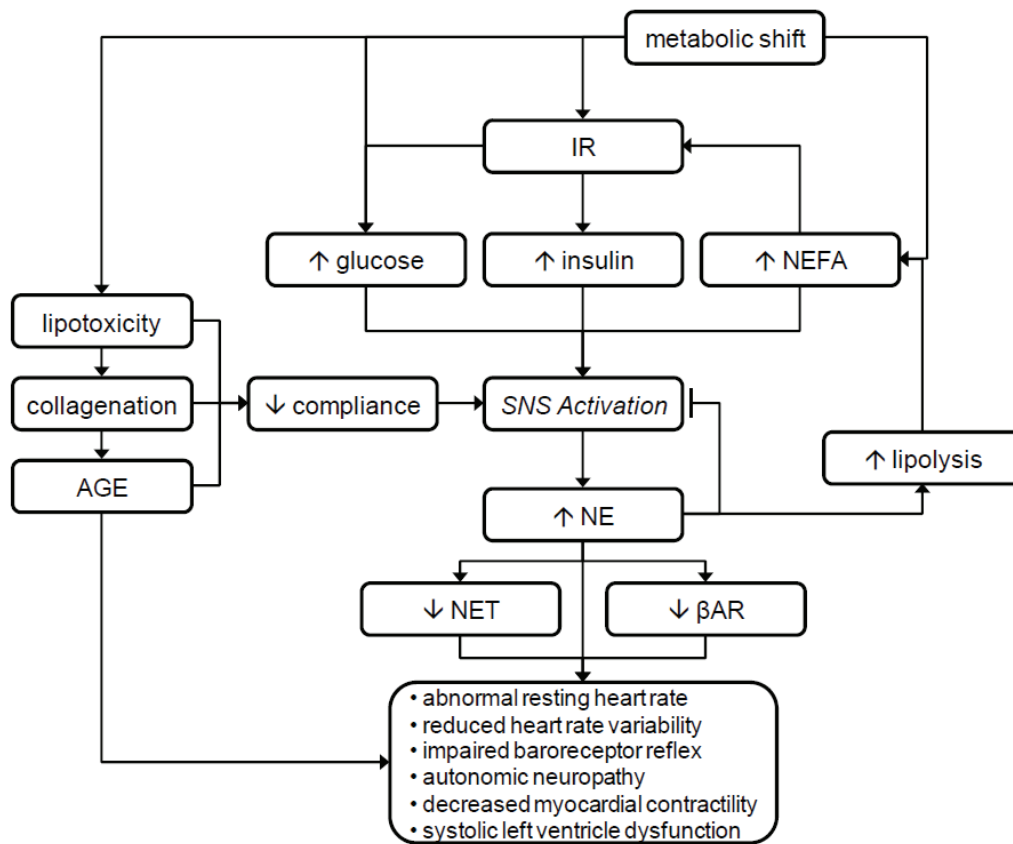
Figure 5. Schematic of sympathetic nervous activation in diabetes and physiological consequences. Shift in myocardial metabolism to fatty acids over glucose stimulate nonesterified fatty acid (NEFA) accumulation and insulin resistance, elevated glucose and insulin levels, and accumulation of lipid metabolites, collagen, and advanced glycation end products (AGE), leading to reduced left ventricular compliance and SNS activation. Chronic elevation of NE leads to downregualtion of NET and β-adrenoceptors with several functional consequences.

cal mechanisms. These studies can be further translated to clinical imaging application, wherein cardiovascular risk may be identified by PET or SPECT.

In addition to established imaging of sympathetic nevous integrity (^{11}C-HED, ^{123}I-MIBG) and β-adrenoceptor density (^{11}C-CGP12177), continuing research can explore novel neurohormonal targets in diabetes. Indirect measurements of cAMP levels by (R)-^{11}C-rolipram may provide a complementary measurement of sympathetic tone in diabetes. While the majority of research to date has focused on the sympathetic signaling axis, changes in parasympathetic neuronal signaling may also play a role in diabetic cardiac risk. Evaluation of myocardial muscarinic receptors using ^{11}C-methylquinuclidinyl benzilate (^{11}C-MQNB) may

provide additional information on cardiac function in diabetes. The development of ^{11}C-labeled angiotensin II type 1 receptor antagonists provide the opportunity for dynamic evaluation of altered angiotensin II signaling, which partially regulates sympathetic tone. Moreover, diabetic patients treated with angiotensin II type 1 receptor blockers have been shown to exhibit improved cardiovascular outcomes.

In the long term, the literature demonstrates that abnormalities in SNS signaling identified using PET and SPECT imaging may be of value in the identification of diabetic patients at greatest risk of cardiac disease, even prior to the development of autonomic neuropathy. Given the link between hyperglycemia and elevated norepinephrine, sympathetic neuronal imaging may be further applied to evaluate myocardial

effects of, and thereby guide, anti-diabetic therapy.

Address correspondence to: Dr. Jean DaSilva, National Cardiac PET Centre, University of Ottawa Heart Institute, 40 Ruskin Street, Ottawa, Ontario, Canada, K1Y 4W7 Tel: 613-798-5555 x 19704; Fax: 613-761-5406; E-mail: JDasilva@ottawaheart.ca

References

[1] Ardell JL. Intrathoracic Neuronal Regulation of Cardiac Function. In: Armour JA, Ardell JL, editors. Basic and Clinical Neurocardiology. New York: Oxford University Press; 2004. p. 118-152.

[2] Crick SJ SMN, Anderson RH. Neural supply of the heart. In: Ter Horst GJ, editors. The nervous system and the heart. Humana Press Inc; 2000. p. 3-54.

[3] Brodde OE, Bruck H and Leineweber K. Cardiac adrenoceptors: physiological and pathophysiological relevance. J Pharmacol Sci 2006; 100: 323-337.

[4] Adams DJ and Cuevas J. Electrophysiological Properties of Intrinsic Cardiac Neurons. In: Armour JA, Ardell JL, editors. Basic and Clinical Neurocardiology. New York: Oxford University Press; 2004. p. 1-60.

[5] Backs J, Haunstetter A, Gerber SH, Metz J, Borst MM, Strasser RH, Kubler W and Haass M. The neuronal norepinephrine transporter in experimental heart failure: evidence for a post-transcriptional downregulation. J Mol Cell Cardiol 2001; 33: 461-472.

[6] Hoffman BB and Lefkowitz RJ. Catecholamines, Sympathomimetic Drugs, and Adrenergic Receptor Antagonists. In: Hardman JGL, Lee E., editors. Goodman & Gilman's The Pharmacological Basis of Therapeutics. Ninth Edition. New York: McGraw-Hill; 1995. p. 199-248.

[7] Hoard JL, Hoover DB, Mabe AM, Blakely RD, Feng N and Paolocci N. Cholinergic neurons of mouse intrinsic cardiac ganglia contain noradrenergic enzymes, norepinephrine transporters, and the neurotrophin receptors tropomyosin-related kinase A and p75. Neuroscience 2008; 156: 129-142.

[8] DaSilva JN, Kilbourn MR and Mangner TJ. Synthesis of [11C]tetrabenazine, a vesicular monoamine uptake inhibitor, for PET imaging studies. App Rad Isot 1993; 44: 673-676.

[9] Raffel D and Wieland D. Assessment of cardiac sympathetic nerve integrity with positron emission tomography. Nucl Med Biol 2001; 28: 541-559.

[10] Taegtmeyer H, McNulty P and Young ME. Adaptation and maladaptation of the heart in diabetes: Part I: general concepts. Circulation 2002; 105: 1727-1733.

[11] Young ME, McNulty P and Taegtmeyer H. Adaptation and maladaptation of the heart in diabetes: Part II: potential mechanisms. Circulation 2002; 105: 1861-1870.

[12] Kerbey AL, Randle PJ, Cooper RH, Whitehouse S, Pask HT and Denton RM. Regulation of pyruvate dehydrogenase in rat heart. Mechanism of regulation of proportions of dephosphorylated and phosphorylated enzyme by oxidation of fatty acids and ketone bodies and of effects of diabetes: role of coenzyme A, acetyl-coenzyme A and reduced and oxidized nicotinamide-adenine dinucleotide. Biochem J 1976; 154: 327-348.

[13] Bruce CR, Hoy AJ, Turner N, Watt MJ, Allen TL, Carpenter K, Cooney GJ, Febbraio MA and Kraegen EW. Overexpression of carnitine palmitoyltransferase-1 in skeletal muscle is sufficient to enhance fatty acid oxidation and improve high-fat diet-induced insulin resistance. Diabetes 2009; 58: 550-558.

[14] Hajduch E, Turban S, Le Liepvre X, Le Lay S, Lipina C, Dimopoulos N, Dugail I and Hundal HS. Targeting of PKCzeta and PKB to caveolin-enriched microdomains represents a crucial step underpinning the disruption in PKB-directed signalling by ceramide. Biochem J 2008; 410: 369-379.

[15] Savage DB, Petersen KF and Shulman GI. Mechanisms of insulin resistance in humans and possible links with inflammation. Hypertension 2005; 45: 828-833.

[16] Huynh K, Kiriazis H, Du XJ, Love JE, Jandeleit-Dahm KA, Forbes JM, McMullen JR and Ritchie RH. Coenzyme Q(10) attenuates diastolic dysfunction, cardiomyocyte hypertrophy and cardiac fibrosis in the db/db mouse model of type 2 diabetes. Diabetologia 2012; 55: 1544-1553.

[17] Wang G, Li W, Lu X and Zhao X. Riboflavin alleviates cardiac failure in Type I diabetic cardiomyopathy. Heart Int 2011; 6: e21.

[18] Norton GR, Candy G and Woodiwiss AJ. Aminoguanidine prevents the decreased myocardial compliance produced by streptozotocin-induced diabetes mellitus in rats. Circulation 1996; 93: 1905-1912.

[19] Candido R, Forbes JM, Thomas MC, Thallas V, Dean RG, Burns WC, Tikellis C, Ritchie RH, Twigg SM, Cooper ME and Burrell LM. A breaker of advanced glycation end products attenuates diabetes-induced myocardial structural changes. Circ Res 2003; 92: 785-792.

[20] Li J, Zhu H, Shen E, Wan L, Arnold JM and Peng T. Deficiency of rac1 blocks NADPH oxidase activation, inhibits endoplasmic reticulum stress, and reduces myocardial remodeling in a mouse model of type 1 diabetes. Diabetes 2010; 59: 2033-2042.

[21] Li Y, Ma J, Zhu H, Singh M, Hill D, Greer PA, Arnold JM, Abel ED and Peng T. Targeted inhibition of calpain reduces myocardial hypertrophy and fibrosis in mouse models of type 1 diabetes. Diabetes 2011; 60: 2985-2994.

[22] Levin BE, Govek EK and Dunn-Meynell AA. Reduced glucose-induced neuronal activation in the hypothalamus of diet-induced obese rats. Brain Res 1998; 808: 317-319.

[23] Ganguly PK, Beamish RE, Dhalla KS, Innes IR and Dhalla NS. Norepinephrine storage, distribution, and release in diabetic cardiomyopathy. Am J Physiol 1987; 252: E734-739.

[24] Thackeray JT, Radziuk J, Harper ME, Suuronen EJ, Ascah KJ, Beanlands RS and Dasilva JN. Sympathetic nervous dysregulation in the absence of systolic left ventricular dysfunction in a rat model of insulin resistance with hyperglycemia. Cardiovasc Diabetol 2011; 10: 75.

[25] Fein FS, Strobeck JE, Malhotra A, Scheuer J and Sonnenblick EH. Reversibility of diabetic cardiomyopathy with insulin in rats. Circ Res 1981; 49: 1251-1261.

[26] Kern W, Peters A, Born J, Fehm HL and Schultes B. Changes in blood pressure and plasma catecholamine levels during prolonged hyperinsulinemia. Metabolism 2005; 54: 391-396.

[27] Florian JP and Pawelczyk JA. Sympathetic and haemodynamic responses to lipids in healthy human ageing. Exp Physiol 2010; 95: 486-497.

[28] Schmidt RE, Dorsey DA, Beaudet LN and Peterson RG. Analysis of the Zucker Diabetic Fatty (ZDF) type 2 diabetic rat model suggests a neurotrophic role for insulin/IGF-I in diabetic autonomic neuropathy. Am J Pathol 2003; 163: 21-28.

[29] Ieda M and Fukuda K. New aspects for the treatment of cardiac diseases based on the diversity of functional controls on cardiac muscles: the regulatory mechanisms of cardiac innervation and their critical roles in cardiac performance. J Pharmacol Sci 2009; 109: 348-353.

[30] Schmid H, Forman LA, Cao X, Sherman PS and Stevens MJ. Heterogeneous cardiac sympathetic denervation and decreased myocardial nerve growth factor in streptozotocin-induced diabetic rats: implications for cardiac sympathetic dysinnervation complicating diabetes. Diabetes 1999; 48: 603-608.

[31] Stevens MJ, Dayanikli F, Raffel DM, Allman KC, Sandford T, Feldman EL, Wieland DM, Corbett J and Schwaiger M. Scintigraphic assessment of regionalized defects in myocardial sympathetic innervation and blood flow regulation in diabetic patients with autonomic neuropathy. J Am Coll Cardiol 1998; 31: 1575-1584.

[32] Ewing DJ, Bellavere F, Espi F, McKibben BM, Buchanan KD, Riemersma RA and Clarke BF. Correlation of cardiovascular and neuroendocrine tests of autonomic function in diabetes. Metabolism 1986; 35: 349-353.

[33] Landsberg L, Saville ME and Young JB. Sympathoadrenal system and regulation of thermogenesis. Am J Physiol 1984; 247: E181-189.

[34] Facchini FS, Stoohs RA and Reaven GM. Enhanced sympathetic nervous system activity. The linchpin between insulin resistance, hyperinsulinemia, and heart rate. Am J Hypertens 1996; 9: 1013-1017.

[35] Jamerson KA, Julius S, Gudbrandsson T, Andersson O and Brant DO. Reflex sympathetic activation induces acute insulin resistance in the human forearm. Hypertension 1993; 21: 618-623.

[36] Jyotsna VP, Sahoo A, Sreenivas V and Deepak KK. Prevalence and pattern of cardiac autonomic dysfunction in newly detected type 2 diabetes mellitus. Diabetes Res Clin Pract 2009; 83: 83-88.

[37] Ganguly PK, Dhalla KS, Innes IR, Beamish RE and Dhalla NS. Altered norepinephrine turnover and metabolism in diabetic cardiomyopathy. Circ Res 1986; 59: 684-693.

[38] Akiyama N, Okumura K, Watanabe Y, Hashimoto H, Ito T, Ogawa K and Satake T. Altered acetylcholine and norepinephrine concentrations in diabetic rat hearts. Role of parasympathetic nervous system in diabetic cardiomyopathy. Diabetes 1989; 38: 231-236.

[39] Marsh SA, Dell'italia LJ and Chatham JC. Interaction of diet and diabetes on cardiovascular function in rats. Am J Physiol Heart Circ Physiol 2009; 296: H282-292.

[40] Marsh SA, Powell PC, Agarwal A, Dell'Italia LJ and Chatham JC. Cardiovascular dysfunction in Zucker obese and Zucker diabetic fatty rats: role of hydronephrosis. Am J Physiol Heart Circ Physiol 2007; 293: H292-298.

[41] Kiyono Y, Iida Y, Kawashima H, Ogawa M, Tamaki N, Nishimura H and Saji H. Norepinephrine transporter density as a causative factor in alterations in MIBG myocardial uptake in NIDDM model rats. Eur J Nucl Med Mol Imaging 2002; 29: 999-1005.

[42] Felten SY, Peterson RG, Shea PA, Besch HR, Jr. and Felten DL. Effects of streptozotocin diabetes on the noradrenergic innervation of the rat heart: a longitudinal histofluorescence and neurochemical study. Brain Res Bull 1982; 8: 593-607.

[43] Gallego M, Setien R, Izquierdo MJ, Casis O and Casis E. Diabetes-induced biochemical changes in central and peripheral catecholaminergic systems. Physiol Res 2003; 52: 735-741.

[44] Patel KP and Zhang PL. Baroreflex function in

streptozotocin (STZ) induced diabetic rats. Diabetes Res Clin Pract 1995; 27: 1-9.

[45] Schreihofer AM, Mandel DA, Mobley SC and Stepp DW. Impairment of sympathetic baroreceptor reflexes in obese Zucker rats. Am J Physiol Heart Circ Physiol 2007; 293: H2543-2549.

[46] Gu H, Epstein PN, Li L, Wurster RD and Cheng ZJ. Functional changes in baroreceptor afferent, central and efferent components of the baroreflex circuitry in type 1 diabetic mice (OVE26). Neuroscience 2008; 152: 741-752.

[47] Borges GR, de Oliveira M, Salgado HC and Fazan R, Jr. Myocardial performance in conscious streptozotocin diabetic rats. Cardiovasc Diabetol 2006; 5: 26.

[48] Kuwahara M, Yayou K, Ishii K, Hashimoto S, Tsubone H and Sugano S. Power spectral analysis of heart rate variability as a new method for assessing autonomic activity in the rat. J Electrocardiol 1994; 27: 333-337.

[49] Ramaekers D, Beckers F, Demeulemeester H and Aubert AE. Cardiovascular autonomic function in conscious rats: a novel approach to facilitate stationary conditions. Ann Noninvasive Electrocardiol 2002; 7: 307-318.

[50] Bertram D, Barres C, Cheng Y and Julien C. Norepinephrine reuptake, baroreflex dynamics, and arterial pressure variability in rats. Am J Physiol Regul Integr Comp Physiol 2000; 279: R1257-1267.

[51] Mills PA, Huetteman DA, Brockway BP, Zwiers LM, Gelsema AJ, Schwartz RS and Kramer K. A new method for measurement of blood pressure, heart rate, and activity in the mouse by radiotelemetry. J Appl Physiol 2000; 88: 1537-1544.

[52] Howarth FC, Jacobson M, Naseer O and Adeghate E. Short-term effects of streptozotocin-induced diabetes on the electrocardiogram, physical activity and body temperature in rats. Exp Physiol 2005; 90: 237-245.

[53] Howarth FC, Jacobson M, Shafiullah M and Adeghate E. Long-term effects of streptozotocin-induced diabetes on the electrocardiogram, physical activity and body temperature in rats. Exp Physiol 2005; 90: 827-835.

[54] Howarth FC, Jacobson M, Shafiullah M and Adeghate E. Effects of insulin treatment on heart rhythm, body temperature and physical activity in streptozotocin-induced diabetic rat. Clin Exp Pharmacol Physiol 2006; 33: 327-331.

[55] Howarth FC, Jacobson M, Shafiullah M and Adeghate E. Long-term effects of type 2 diabetes mellitus on heart rhythm in the Goto-Kakizaki rat. Exp Physiol 2008; 93: 362-369.

[56] Kiyono Y, Kanegawa N, Kawashima H, Iida Y, Kinoshita T, Tamaki N, Nishimura H, Ogawa M and Saji H. Age-related changes of myocardial norepinephrine transporter density in rats: implications for differential cardiac accumulation of MIBG in aging. Nucl Med Biol 2002; 29: 679-684.

[57] Hekimian G, Khandoudi N, Feuvray D and Beigelman PM. Abnormal cardiac rhythm in diabetic rats. Life Sci 1985; 37: 547-551.

[58] Chen L, Wang L, Xu B, Ni G, Yu L, Han B, Yu X, Wang K, Lai Y, Zhou S and Zhu Q. Mechanisms of alpha1-adrenoceptor mediated QT prolongation in the diabetic rat heart. Life Sci 2009; 84: 250-256.

[59] Gallego M and Casis O. Regulation of cardiac transient outward potassium current by norepinephrine in normal and diabetic rats. Diabetes Metab Res Rev 2001; 17: 304-309.

[60] Goncalves AC, Tank J, Diedrich A, Hilzendeger A, Plehm R, Bader M, Luft FC, Jordan J and Gross V. Diabetic hypertensive leptin receptor-deficient db/db mice develop cardioregulatory autonomic dysfunction. Hypertension 2009; 53: 387-392.

[61] Gross V, Tank J, Partke HJ, Plehm R, Diedrich A, da Costa Goncalves AC, Luft FC and Jordan J. Cardiovascular autonomic regulation in Non-Obese Diabetic (NOD) mice. Auton Neurosci 2008; 138: 108-113.

[62] Fazan R Jr, Ballejo G, Salgado MC, Moraes MF and Salgado HC. Heart rate variability and baroreceptor function in chronic diabetic rats. Hypertension 1997; 30: 632-635.

[63] Flaa A, Aksnes TA, Kjeldsen SE, Eide I and Rostrup M. Increased sympathetic reactivity may predict insulin resistance: an 18-year follow-up study. Metabolism 2008; 57: 1422-1427.

[64] Carnethon MR, Golden SH, Folsom AR, Haskell W and Liao D. Prospective investigation of autonomic nervous system function and the development of type 2 diabetes: the Atherosclerosis Risk In Communities study, 1987-1998. Circulation 2003; 107: 2190-2195.

[65] Bristow MR. Changes in myocardial and vascular receptors in heart failure. J Am Coll Cardiol 1993; 22: 61A-71A.

[66] Dell'Italia LJ and Ardell JL. Sympathetic Nervous System in the Evolution of Heart Failure. In: Armour JA, Ardell JL, editors. Basic and Clinical Neurocardiology. New York: Oxford University Press; 2004. p. 340-367.

[67] Dincer UD, Bidasee KR, Guner S, Tay A, Ozcelikay AT and Altan VM. The effect of diabetes on expression of beta1-, beta2-, and beta3-adrenoreceptors in rat hearts. Diabetes 2001; 50: 455-461.

[68] Sellers DJ and Chess-Williams R. The effect of streptozotocin-induced diabetes on cardiac beta-adrenoceptor subtypes in the rat. J Auton Pharmacol 2001; 21: 15-21.

[69] Avendano GF, Agarwal RK, Bashey RI, Lyons MM, Soni BJ, Jyothirmayi GN and Regan TJ. Effects of glucose intolerance on myocardial function and collagen-linked glycation. Diabetes 1999; 48: 1443-1447.

[70] Swan JW, Anker SD, Walton C, Godsland IF,

Clark AL, Leyva F, Stevenson JC and Coats AJ. Insulin resistance in chronic heart failure: relation to severity and etiology of heart failure. J Am Coll Cardiol 1997; 30: 527-532.

[71] Atkins FL, Dowell RT and Love S. beta-Adrenergic receptors, adenylate cyclase activity, and cardiac dysfunction in the diabetic rat. J Cardiovasc Pharmacol 1985; 7: 66-70.

[72] Matsuda N, Hattori Y, Gando S, Akaishi Y, Kemmotsu O and Kanno M. Diabetes-induced down-regulation of beta1-adrenoceptor mRNA expression in rat heart. Biochem Pharmacol 1999; 58: 881-885.

[73] Beenen OH, Batink HD, Pfaffendorf M and van Zwieten PA. Beta-andrenoceptors in the hearts of diabetic-hypertensive rats: radioligand binding and functional experiments. Blood Press 1997; 6: 44-51.

[74] Ingebretsen CG, Hawelu-Johnson C and Ingebretsen WR Jr. Alloxan-induced diabetes reduces beta-adrenergic receptor number without affecting adenylate cyclase in rat ventricular membranes. J Cardiovasc Pharmacol 1983; 5: 454-461.

[75] Latifpour J and McNeill JH. Cardiac autonomic receptors: effect of long-term experimental diabetes. J Pharmacol Exp Ther 1984; 230: 242-249.

[76] Kashiwagi A, Nishio Y, Saeki Y, Kida Y, Kodama M and Shigeta Y. Plasma membrane-specific deficiency in cardiac beta-adrenergic receptor in streptozocin-diabetic rats. Am J Physiol 1989; 257: E127-132.

[77] Sharma V, Parsons H, Allard MF and McNeill JH. Metoprolol increases the expression of beta(3)-adrenoceptors in the diabetic heart: effects on nitric oxide signaling and forkhead transcription factor-3. Eur J Pharmacol 2008; 595: 44-51.

[78] Sharma V, Dhillon P, Wambolt R, Parsons H, Brownsey R, Allard MF and McNeill JH. Metoprolol improves cardiac function and modulates cardiac metabolism in the streptozotocin-diabetic rat. Am J Physiol Heart Circ Physiol 2008; 294: H1609-1620.

[79] Sharma V, Dhillon P, Parsons H, Allard MF and McNeill JH. Metoprolol represses PGC1alpha-mediated carnitine palmitoyltransferase-1B expression in the diabetic heart. Eur J Pharmacol 2009; 607: 156-166.

[80] Gotzsche O. The adrenergic beta-receptor adenylate cyclase system in heart and lymphocytes from streptozotocin-diabetic rats. In vivo and in vitro evidence for a desensitized myocardial beta-receptor. Diabetes 1983; 32: 1110-1116.

[81] Gando S, Hattori Y, Akaishi Y, Nishihira J and Kanno M. Impaired contractile response to beta adrenoceptor stimulation in diabetic rat hearts: alterations in beta adrenoceptors-G protein-adenylate cyclase system and phospholamban phosphorylation. J Pharmacol Exp Ther 1997; 282: 475-484.

[82] op den Buijs J, Miklos Z, van Riel NA, Prestia CM, Szenczi O, Toth A, Van der Vusse GJ, Szabo C, Ligeti L and Ivanics T. beta-Adrenergic activation reveals impaired cardiac calcium handling at early stage of diabetes. Life Sci 2005; 76: 1083-1098.

[83] Yoshinaga K, Chow BJ, deKemp R, Thorn S, Ruddy T, Davies RA, DaSilva J and Beanlands R. Application of cardiac molecular imaging using positron emission tomography in evaluation of drug and therapeutics for cardiovascular disorders. Curr Pharm Des 2005; 11: 903-932.

[84] Delahaye N, Le Guludec D, Dinanian S, Delforge J, Slama MS, Sarda L, Dolle F, Mzabi H, Samuel D, Adams D, Syrota A and Merlet P. Myocardial muscarinic receptor upregulation and normal response to isoproterenol in denervated hearts by familial amyloid polyneuropathy. Circulation 2001; 104: 2911-2916.

[85] Hadizad T, Kirkpatrick SA, Mason S, Burns K, Beanlands RS and Dasilva JN. Novel O-[(11)C] methylated derivatives of candesartan as angiotensin II AT(1) receptor imaging ligands: radiosynthesis and ex vivo evaluation in rats. Bioorg Med Chem 2009; 17: 7971-7977.

[86] Higuchi T, Fukushima K, Xia J, Mathews WB, Lautamaki R, Bravo PE, Javadi MS, Dannals RF, Szabo Z and Bengel FM. Radionuclide imaging of angiotensin II type 1 receptor upregulation after myocardial ischemia-reperfusion injury. J Nucl Med 2010; 51: 1956-1961.

[87] DaSilva JN, Lourenco CM, Meyer JH, Hussey D, Potter WZ and Houle S. Imaging cAMP-specific phosphodiesterase-4 in human brain with (R)-[11C]rolipram and positron emission tomography. Eur J Nucl Med Mol Imaging 2002; 29: 1680-1683.

[88] Otani H, Kagaya Y, Imahori Y, Yasuda S, Fujii R, Chida M, Namiuchi S, Takeda M, Sakuma M, Watanabe J, Ido T, Nonogi H and Shirato K. Myocardial 11C-diacylglycerol accumulation and left ventricular remodeling in patients after myocardial infarction. J Nucl Med 2005; 46: 553-559.

[89] Kenk M, Thomas AJ, Lortie M, deKemp RA, Beanlands RS and DaSilva JN. PET Measurements of cAMP-Mediated Phosphodiesterase-4 with (R)-[11C]Rolipram. Current Radiopharmaceuticals 2011; 4: 44-58.

[90] Jacobson AF, Senior R, Cerqueira MD, Wong ND, Thomas GS, Lopez VA, Agostini D, Weiland F, Chandna H and Narula J. Myocardial iodine-123 meta-iodobenzylguanidine imaging and cardiac events in heart failure. Results of the prospective ADMIRE-HF (AdreView Myocardial Imaging for Risk Evaluation in Heart Failure) study. J Am Coll Cardiol 2010; 55: 2212-2221.

[91] Bravo PE and Bengel FM. The Role of Cardiac PET in Translating Basic Science into the Clinical Arena. J Cardiovasc Transl Res 2011; 4: 425-436.

[92] Lautamaki R, Tipre D and Bengel FM. Cardiac sympathetic neuronal imaging using PET. Eur J Nucl Med Mol Imaging 2007; 34 Suppl 1: S74-85.

[93] Tipre DN, Fox JJ, Holt DP, Green G, Yu J, Pomper M, Dannals RF and Bengel FM. In vivo PET imaging of cardiac presynaptic sympathoneuronal mechanisms in the rat. J Nucl Med 2008; 49: 1189-1195.

[94] DeGrado TR, Hutchins GD, Toorongian SA, Wieland DM, Schwaiger M. Myocardial Kinetics of Carbon-11-Meta-Hydroxyephedrine: Retention Mechanisms and Effects of Norepinephrine. J Nucl Med 1993; 34: 1287-1293.

[95] Dae MW, De Marco T, Botvinick EH, O'Connell JW, Hattner RS, Huberty JP and Yuen-Green MS. Scintigraphic assessment of MIBG uptake in globally denervated human and canine hearts--implications for clinical studies. J Nucl Med 1992; 33: 1444-1450.

[96] Kasama S, Toyama T, Sumino H, Kumakura H, Takayama Y, Ichikawa S, Suzuki T and Kurabayashi M. Long-term nicorandil therapy improves cardiac sympathetic nerve activity after reperfusion therapy in patients with first acute myocardial infarction. J Nucl Med 2007; 48: 1676-1682.

[97] Kasama S, Toyama T, Sumino H, Kumakura H, Takayama Y, Minami K, Ichikawa S, Matsumoto N, Sato Y and Kurabayashi M. Prognostic value of cardiac sympathetic nerve activity evaluated by [123I]m-iodobenzylguanidine imaging in patients with ST-segment elevation myocardial infarction. Heart 2011; 97: 20-26.

[98] Boogers MJ, Borleffs CJ, Henneman MM, van Bommel RJ, van Ramshorst J, Boersma E, Dibbets-Schneider P, Stokkel MP, van der Wall EE, Schalij MJ and Bax JJ. Cardiac sympathetic denervation assessed with 123-iodine metaiodobenzylguanidine imaging predicts ventricular arrhythmias in implantable cardioverter-defibrillator patients. J Am Coll Cardiol 2010; 55: 2769-2777.

[99] Bax JJ, Kraft O, Buxton AE, Fjeld JG, Parizek P, Agostini D, Knuuti J, Flotats A, Arrighi J, Muxi A, Alibelli MJ, Banerjee G and Jacobson AF. 123 I-mIBG scintigraphy to predict inducibility of ventricular arrhythmias on cardiac electrophysiology testing: a prospective multicenter pilot study. Circ Cardiovasc Imaging 2008; 1: 131-140.

[100] Currie GM, Iqbal B, Wheat JM, Wang L, Trifunovic M, Jelinek HF and Kiat H. Risk Stratification in Heart Failure Using 123I-MIBG. J Nucl Med Technol 2011; 39: 295-301.

[101] Narula J and Sarkar K. A conceptual paradox of MIBG uptake in heart failure: retention with incontinence! J Nucl Cardiol 2003; 10: 700-704.

[102] Raffel DM and Chen W. Binding of [3H] mazindol to cardiac norepinephrine transporters: kinetic and equilibrium studies. Naunyn Schmiedebergs Arch Pharmacol 2004; 370: 9-16.

[103] Wieland DM, Rosenspire KC, Hutchins GD, Van Dort M, Rothley JM, Mislankar SG, Lee HT, Massin CC, Gildersleeve DL, Sherman PS and et al. Neuronal mapping of the heart with 6-[18F]fluorometaraminol. J Med Chem 1990; 33: 956-964.

[104] Fuller RW, Snoddy HD, Perry KW, Bernstein JR and Murphy PJ. Formation of alpha-methylnorepinephrine as a metabolite of metaraminol in guinea pigs. Biochem Pharmacol 1981; 30: 2831-2836.

[105] Thackeray JT, Beanlands RS and Dasilva JN. Presence of Specific 11C-meta-Hydroxyephedrine Retention in Heart, Lung, Pancreas, and Brown Adipose Tissue. J Nucl Med 2007; 48: 1733-1740.

[106] Rosenspire KC, Haka MS, Van Dort ME, Jewett DM, Gildersleeve DL, Schwaiger M and Wieland DM. Synthesis and preliminary Evaluation of Carbon-11-Meta-Hydroxyephedrine: A False Transmitter Agent for Heart Neuronal Imaging. J Nucl Med 1990; 31: 1328-1334.

[107] Law MP, Osman S, Davenport RJ, Cunningham VJ, Pike VW and Camici PG. Biodistribution and metabolism of [N-methyl-11C]m-hydroxyephedrine in the rat. Nucl Med Biol 1997; 24: 417-424.

[108] Caldwell JH, Kroll K, Li Z, Seymour K, Link JM and Krohn KA. Quantitation of presynaptic cardiac sympathetic function with carbon-11-meta-hydroxyephedrine. J Nucl Med 1998; 39: 1327-1334.

[109] Law MP, Schafers K, Kopka K, Wagner S, Schober O and Schafers M. Molecular imaging of cardiac sympathetic innervation by 11C-mHED and PET: from man to mouse? J Nucl Med 2010; 51: 1269-1276.

[110] Allman KC, Wieland DM, Muzik O, Degrado TR, Wolfe ER, Jr. and Schwaiger M. Carbon-11 hydroxyephedrine with positron emission tomography for serial assessment of cardiac adrenergic neuronal function after acute myocardial infarction in humans. J Am Coll Cardiol 1993; 22: 368-375.

[111] Bengel FM, Ueberfuhr P, Hesse T, Schiepel N, Ziegler SI, Scholz S, Nekolla SG, Reichart B and Schwaiger M. Clinical determinants of ventricular sympathetic reinnervation after orthotopic heart transplantation. Circulation 2002; 106: 831-835.

[112] Schwaiger M, Hutchins GD, Kalff V, Rosenspire K, Haka MS, Mallette S, Deeb GM, Abrams GD and Wieland D. Evidence for regional catecholamine uptake and storage sites in the transplanted human heart by positron emission tomography. J Clin Invest 1991; 87: 1681-1690.

[113] Kies P, Wichter T, Schafers M, Paul M, Schafers KP, Eckardt L, Stegger L, Schulze-Bahr E, Rimoldi O, Breithardt G, Schober O and Camici PG. Abnormal myocardial presynaptic norepinephrine recycling in patients with Brugada syndrome. Circulation 2004; 110: 3017-3022.

[114] Sasano T, Abraham MR, Chang KC, Ashikaga H, Mills KJ, Holt DP, Hilton J, Nekolla SG, Dong J, Lardo AC, Halperin H, Dannals RF, Marban E and Bengel FM. Abnormal sympathetic innervation of viable myocardium and the substrate of ventricular tachycardia after myocardial infarction. J Am Coll Cardiol 2008; 51: 2266-2275.

[115] Hartmann F, Ziegler S, Nekolla S, Hadamitzky M, Seyfarth M, Richardt G and Schwaiger M. Regional patterns of myocardial sympathetic denervation in dilated cardiomyopathy: an analysis using carbon-11 hydroxyephedrine and positron emission tomography. Heart 1999; 81: 262-270.

[116] Ungerer M, Bohm M, Elce JS, Erdmann E and Lohse MJ. Altered expression of beta-adrenergic receptor kinase and beta 1-adrenergic receptors in the failing human heart. Circulation 1993; 87: 454-463.

[117] Ungerer M, Weig HJ, Kubert S, Overbeck M, Bengel F, Schomig A and Schwaiger M. Regional pre- and postsynaptic sympathetic system in the failing human heart--regulation of beta ARK-1. Eur J Heart Fail 2000; 2: 23-31.

[118] Luisi AJ, Fallavollita JA, Suzuki G, deKemp R, Haka MS, Toorongian SA and Canty JM Jr. Regional 11C-Hydroxyephedrine Uptake in Hibernating Myocardium: Chronic Inhomogeneity of Sympathetic Innervation in the Absence of Infarction. J Nucl Med 2005; 46: 1368-1374.

[119] John AS, Mongillo M, Depre C, Khan MT, Rimoldi OE, Pepper JR, Dreyfus GD, Pennell DJ and Camici PG. Pre- and post-synaptic sympathetic function in human hibernating myocardium. Eur J Nucl Med Mol Imaging 2007; 34: 1973-1980.

[120] Schafers M, Dutka D, Rhodes CG, Lammertsma AA, Hermansen F, Schober O and Camici PG. Myocardial presynaptic and postsynaptic autonomic dysfunction in hypertrophic cardiomyopathy. Circ Res 1998; 82: 57-62.

[121] Bulow HP, Stahl F, Lauer B, Nekolla SG, Schuler G, Schwaiger M and Bengel FM. Alterations of myocardial presynaptic sympathetic innervation in patients with multi-vessel coronary artery disease but without history of myocardial infarction. Nucl Med Commun 2003; 24: 233-239.

[122] Del Rosario RB, Jung Y-W, Caraher J, Chakraborty PK and Wieland DM. Synthesis and Preliminary Evaluation of [^{11}C]-(-)-Phenylephrine as a Functional Heart Neuronal PET Agent. Nucl Med Biol 1996; 23: 611-616.

[123] Nguyen NT, DeGrado TR, Chakraborty P, Wieland DM and Schwaiger M. Myocardial kinetics of carbon-11-epinephrine in the isolated working rat heart. J Nucl Med 1997; 38: 780-785.

[124] Mohell N and Dicker A. The beta-adrenergic radioligand [3H]CGP-12177, generally classified as an antagonist, is a thermogenic agonist in brown adipose tissue. Biochem J 1989; 261: 401-405.

[125] Affolter H, Hertel C, Jaeggi K, Portenier M and Staehelin M. (-)-S-[3H]CGP-12177 and its use to determine the rate constants of unlabeled beta-adrenergic antagonists. Proc Natl Acad Sci USA 1985; 82: 925-929.

[126] Van Waarde A, Elsinga PH, Brodde O-E, Visser GM and Vaalburg W. Myocardial and pulmonary uptake of S-1'[^{18}F]fluorocarazolol in intact rats reflects radioligand binding to ß-adrenoceptors. European Journal of Pharmacology 1995; 272: 159-168.

[127] Thackeray JT, Parsa-Nezhad M, Kenk M, Thorn SL, Kolajova M, Beanlands RS and Dasilva JN. Reduced CGP12177 binding to cardiac beta-adrenoceptors in hyperglycemic high-fat-diet-fed, streptozotocin-induced diabetic rats. Nucl Med Biol 2011; 38: 1059-1066.

[128] Link JM, Stratton JR, Levy W, Poole JE, Shoner SC, Stuetzle W and Caldwell JH. PET measures of pre- and post-synaptic cardiac beta adrenergic function. Nucl Med Biol 2003; 30: 795-803.

[129] Caldwell JH, Link JM, Levy WC, Poole JE and Stratton JR. Evidence for pre- to postsynaptic mismatch of the cardiac sympathetic nervous system in ischemic congestive heart failure. J Nucl Med 2008; 49: 234-241.

[130] Naya M, Tsukamoto T, Morita K, Katoh C, Nishijima K, Komatsu H, Yamada S, Kuge Y, Tamaki N and Tsutsui H. Myocardial beta-adrenergic receptor density assessed by 11C-CGP12177 PET predicts improvement of cardiac function after carvedilol treatment in patients with idiopathic dilated cardiomyopathy. J Nucl Med 2009; 50: 220-225.

[131] Tsukamoto T, Morita K, Naya M, Inubushi M, Katoh C, Nishijima K, Kuge Y, Okamoto H, Tsutsui H and Tamaki N. Decreased myocardial beta-adrenergic receptor density in relation to increased sympathetic tone in patients with nonischemic cardiomyopathy. J Nucl Med 2007; 48: 1777-1782.

[132] Lortie M, DaSilva JN, Kenk M, Thorn S, Davis D, Birnie D, Beanlands RS and deKemp RA. Analysis of (R)- and (S)-[(11)C]rolipram kinetics in canine myocardium for the evaluation of phosphodiesterase-4 with PET. Mol Imaging Biol 2012; 14: 225-236.

[133] Thomas AJ, DaSilva JN, Lortie M, Renaud JM, Kenk M, Beanlands RS and deKemp RA. PET of (R)-11C-rolipram binding to phosphodiesterase-4 is reproducible and sensitive to increased norepinephrine in the rat heart. J Nucl Med 2011; 52: 263-269.

[134] Kenk M, Greene M, Thackeray J, Dekemp RA, Lortie M, Thorn S, Beanlands RS and Dasilva JN. In vivo selective binding of (R)-[(11)C] rolipram to phosphodiesterase-4 provides the

basis for studying intracellular cAMP signaling in the myocardium and other peripheral tissues. Nucl Med Biol 2007; 34: 71-77.

[135] Kenk M, Thackeray JT, Thorn SL, Dhami K, Chow BJ, Ascah KJ, Dasilva JN and Beanlands RS. Alterations of pre- and postsynaptic noradrenergic signaling in a rat model of adriamycin-induced cardiotoxicity. J Nucl Cardiol 2010; 17: 175-176.

[136] Greene M, Thackeray JT, Kenk M, Thorn SL, Bevilacqua L, Harper M-E, Beanlands RS and DaSilva JN. Reduced *In Vivo* Phosphodiesterase -4 Response to Norepinephrine Challenge in Diet-Induced Obese Rats. Can J Physiol Pharmacol 2009; 87: 196-202.

[137] Kusmic C, Morbelli S, Marini C, Matteucci M, Cappellini C, Pomposelli E, Marzullo P, L'Abbate A and Sambuceti G. Whole-body evaluation of MIBG tissue extraction in a mouse model of long-lasting type II diabetes and its relationship with norepinephrine transport protein concentration. J Nucl Med 2008; 49: 1701-1706.

[138] Goethals LR, Weytjens CD, De Geeter F, Droogmans S, Caveliers V, Keyaerts M, Vanhove C, Van Camp G, Bossuyt A and Lahoutte T. Regional quantitative analysis of small animal myocardial sympathetic innervation and initial application in streptozotocin induced diabetes. Contrast Media Mol Imaging 2009; 4: 174-182.

[139] Dubois EA, Kam KL, Somsen GA, Boer GJ, de Bruin K, Batink HD, Pfaffendorf M, van Royen EA and van Zwieten PA. Cardiac iodine-123 metaiodobenzylguanidine uptake in animals with diabetes mellitus and/or hypertension. Eur J Nucl Med 1996; 23: 901-908.

[140] Kiyono Y, Iida Y, Kawashima H, Tamaki N, Nishimura H and Saji H. Regional alterations of myocardial norepinephrine transporter density in streptozotocin-induced diabetic rats: implications for heterogeneous cardiac accumulation of MIBG in diabetes. Eur J Nucl Med 2001; 28: 894-899.

[141] Gerson MC, Caldwell JH, Ananthasubramaniam K, Clements IP, Henzlova MJ, Amanullah A and Jacobson AF. Influence of diabetes mellitus on prognostic utility of imaging of myocardial sympathetic innervation in heart failure patients. Circ Cardiovasc Imaging 2011; 4: 87-93.

[142] Takahashi N, Nakagawa M, Saikawa T, Ooie T, Yufu K, Shigematsu S, Hara M, Sakino H, Katsuragi I, Okeda T, Yoshimatsu H and Sakata T. Effect of essential hypertension on cardiac autonomic function in type 2 diabetic patients. J Am Coll Cardiol 2001; 38: 232-237.

[143] Sacre JW, Franjic B, Jellis CL, Jenkins C, Coombes JS and Marwick TH. Association of cardiac autonomic neuropathy with subclinical myocardial dysfunction in type 2 diabetes. JACC Cardiovasc Imaging 2010; 3: 1207-1215.

[144] Stevens MJ, Raffel DM, Allman KC, Schwaiger M and Wieland DM. Regression and progression of cardiac sympathetic dysinnervation complicating diabetes: an assessment by C-11 hydroxyephedrine and positron emission tomography. Metabolism 1999; 48: 92-101.

[145] Muhr-Becker D, Weiss M, Tatsch K, Wolfram G, Standl E and Schnell O. Scintigraphically assessed cardiac sympathetic dysinnervation in poorly controlled type 1 diabetes mellitus: one-year follow-up with improved metabolic control. Exp Clin Endocrinol Diabetes 1999; 107: 306-312.

[146] Fricke E, Eckert S, Dongas A, Fricke H, Preuss R, Lindner O, Horstkotte D and Burchert W. Myocardial sympathetic innervation in patients with symptomatic coronary artery disease: follow-up after 1 year with neurostimulation. J Nucl Med 2008; 49: 1458-1464.

[147] Pop-Busui R, Kirkwood I, Schmid H, Marinescu V, Schroeder J, Larkin D, Yamada E, Raffel DM and Stevens MJ. Sympathetic dysfunction in type 1 diabetes: association with impaired myocardial blood flow reserve and diastolic dysfunction. J Am Coll Cardiol 2004; 44: 2368-2374.

[148] Cohn JN, Levine TB, Olivari MT, Garberg V, Lura D, Francis GS, Simon AB and Rector T. Plasma norepinephrine as a guide to prognosis in patients with chronic congestive heart failure. N Engl J Med 1984; 311: 819-823.